Computer Simulation of Small-Signal and Noise Behavior of Microwave Bipolar Transistors Up to 12 GHz

KARL HARTMANN, MEMBER, IEEE, AND MAX J. O. STRUTT, FELLOW, IEEE

Abstract—**Computer-aided determination and optimization of lumped elements of equivalent circuits based on experimental data, application to the lumped equivalent circuit including noise sources of microwave bipolar transistors, and calculation of gain, noise, and stability from the said computer simulation are dealt with. As an example, a special microwave transistor mount and aspects of a new rugged metal–ceramic package are considered.**

I. Introduction

IMPROVEMENT of the microwave bipolar transistors can only be made by intricate technological processes. Not only the chip itself should be improved, but also the package.

In this paper, different computer simulation methods are described and compared, allowing the determination of equivalent circuits containing lumped elements. In this connection, the sensitivity calculations by Director and Rohrer [1], Goddard and Spence [2], and Downs [16] are compared. The equivalent circuit of a bipolar transistor up to 12 GHz is described. Furthermore, the influence of the circuit elements is shown, thus obtaining several new aspects for microwave transistor construction.

II. Transistor Equivalent Circuit

The determination of the equivalent circuit is based on the measured scattering and noise parameters [3], [27]. The transistor fixture used is shown in Fig. 1. This transistor mount shows a better VSWR and smaller losses than the presently known stripline mounts. At 14 GHz, the VSWR is 1.20 and the loss is 0.17 dB (sum of both ports). These values were measured with joined ports.

As an example, the equivalent circuit for the microwave bipolar transistor AT-561 at the bias condition (I_C = 3 mA, U_{CE} = 10 V) will be determined. This transistor shows a small metallization area resulting in small parasitic capacitances. The chip is bonded to a rugged metal–ceramic package.

Different variants of models describing transistor behavior are known, such as physical models, blackbox models, tables, mathematical models, and equivalent network models. Not all of these models provide the same insight into the device behavior, as stressed by Villalaz [4]. Good device models are amenable to analysis by computer, but they must be related to the semiconductor morphology and the physical processes.

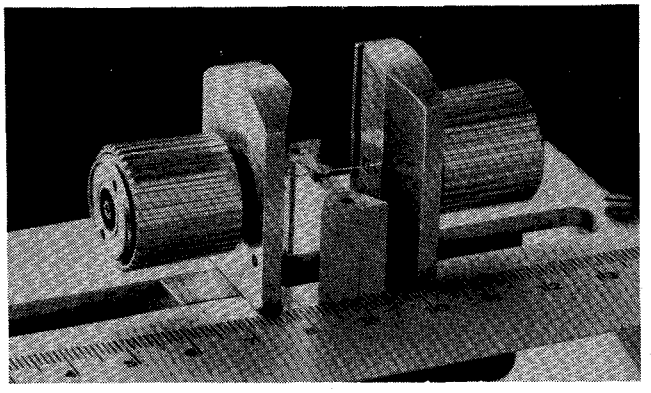

Fig. 1. Coaxial transistor mount for frequencies up to 15 GHz (scale in centimeters).

In this paper, the equivalent circuit of Fig. 2 is applied. In [5] the branch containing the capacitance $C_{b'e'}$ shows a serial resistance with a very small value compared with $|1/\omega C_{b'e'}|$. This is also true for the present new transistor in the higher frequency range. For this reason, this resistance is omitted. The base resistance is divided up into two parts. One part takes into consideration the outer base, the other the inner base, resulting in a better approximation of the small-signal parameters. The derivation of the package equivalent circuit is given in [6].

Since the computer time increases rapidly with the number of network elements and since the connections to the transistor morphology become more complex, the transistor model should be as simple as possible.

In Fig. 2 the noise sources are also introduced [7]. It is one aim of this paper to see if this noise theory gives satisfactory agreement with the measurement at frequencies above 8 GHz [9]. The four noise parameters (Y_{opt},F_{opt},R_n) have therefore not been used for the computer-aided determination of the small-signal equivalent circuit. But at the end of this optimization, the noise parameters have been calculated. They are then compared with the experimental results in Section V. In [8] the experimental verification of the theory has been presented below 4 GHz, while here this verification extends to 10.5 GHz.

III. Computer-Aided Determination of the Equivalent Circuits

As many network analyses have to be executed during the equivalent network determination, it is important to use efficient computer methods. For time-saving network

Manuscript received February 12, 1973; revised August 20, 1973.

K. Hartmann was with the Department of Advanced Electrical Engineering, Swiss Federal Institute of Technology, Zurich, Switzerland. He is now with Brown Boveri Research Center, Daettwil, Switzerland.

M. J. O. Strutt is with the Department of Advanced Electrical Engineering, Swiss Federal Institute of Technology, Zurich, Switzerland.

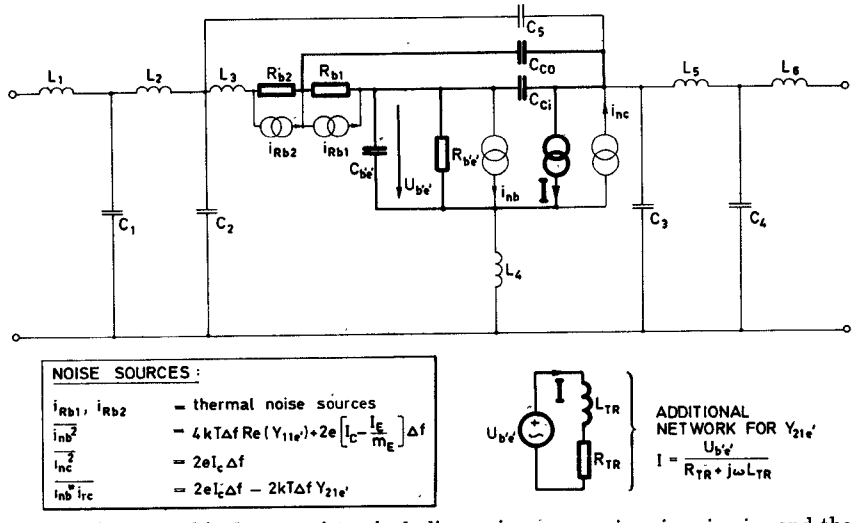

Fig. 2. Equivalent circuit of a microwave bipolar transistor including noise sources i_{Rb1}, i_{Rb2}, i_{nb}, i_{nc}, and the additional network for the complex transadmittance, including the signal current source I.

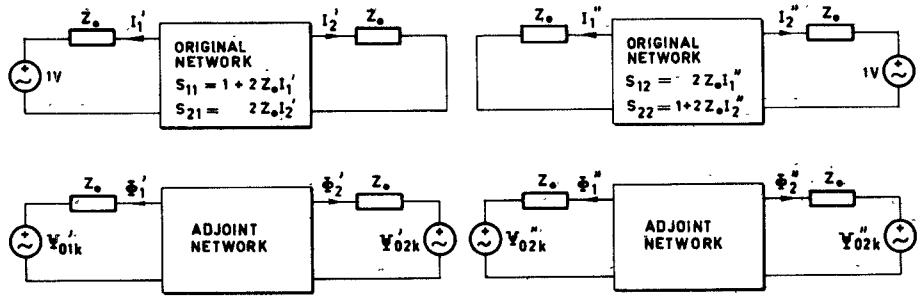

Fig. 3. Original and adjoint networks for the direct sensitivity computation for the s parameters.

analysis, it is imperative to inquire whether the electrical quantities should be calculated either using orthogonal Kirchhoff modes [10], or using a general computer method of matrix inversion making use of generally valid mathematical expressions instead of numerical values, or using ECAP and comparable methods.

This paper is based on an extended ECAP solution. The equivalent circuit may be found by varying the network elements at a fixed topology until the calculated parameters agree sufficiently with the measured ones, applying computer optimization [17]. These methods make sense because in many cases not all the elements of the chosen model can be calculated with sufficient precision using well-known formulas based on physical simplification (e.g., see transadmittance in Section IV).

At first, a comparison of two sensitivity determinations [1], [2] is given. Many optimization methods are based on the gradient calculation, especially using accurate starting values.

Usually, the scattering parameters are used as small-signal parameters in the microwave range. In [5] the objective function is formed with input and output currents of the two-ports showing a relationship with the s parameters (Fig. 3). In this paper, the sensitivity calculation is carried out directly using scattering parameters. As the determination of the error function for the s_{11} and s_{21} parameters is analogous to that for the other two s parameters, only the procedure for the first said error function is described. This function is expressed by (1):

$$E_1 = \int_{\omega_1}^{\omega_2} \frac{1}{n} \{W_{1(j\omega)} \mid s_{11(j\omega)} - \hat{s}_{11(j\omega)} \mid^n + W_{2(j\omega)} \mid s_{21(j\omega)} - \hat{s}_{21(j\omega)} \mid^n\} d\omega \quad (1)$$

where

$W_{i(j\omega)}$	weight functions (real and nonnegative);
$\wedge$	measured value;
n	integer number; in our case $n = 2$;
ω_1 resp ω_2	lower resp. upper angular frequency value.

The first-order sensitivity related to an equivalent network element (El) is

$$\frac{\partial E_1}{\partial El} = \int_{\omega_1}^{\omega_2} \mathrm{Re}\left\{W_{1(j\omega)} \mid s_{11(j\omega)} - \hat{s}_{11(j\omega)} \mid^{n-2} \cdot (s_{11(j\omega)}^* - \hat{s}_{11(j\omega)}^*) \frac{s_{11(j\omega)}}{\partial El} + W_{2(j\omega)} \mid s_{21(j\omega)} - \hat{s}_{21(j\omega)} \mid^{n-2} \cdot (s_{21(j\omega)}^* - \hat{s}_{21(j\omega)}^*) \frac{s_{21(j\omega)}}{\partial El}\right\} d\omega \quad (2)$$

where * is the complex-conjugate value. With the sign convention of Fig. 3 it can be seen that

$$\frac{\partial s_{11(j\omega)}}{\partial E1} = 2Z_0 \frac{\partial I_{1(j\omega)}'}{\partial El} \quad (3)$$

$$\frac{\partial s_{21(j\omega)}}{\partial E1} = 2Z_0 \frac{\partial I_{2(j\omega)}'}{\partial El}. \tag{4}$$

Using the method [1], the error sources of (5) and (6) have to be applied at the ports of the adjoint two-port. Z_0 is the characteristic impedance:

$$\psi_{01(j\omega)}' = -2Z_0 W_{1(j\omega)} \mid s_{11(j\omega)} - \hat{s}_{11(j\omega)} \mid^{n-2} (s_{11(j\omega)}^* - \hat{s}_{11(j\omega)}^*) \tag{5}$$

$$\psi_{02(j\omega)}' = -2Z_0 W_{2(j\omega)} \mid s_{21(j\omega)} - \hat{s}_{21(j\omega)} \mid^{n-2} (s_{21(j\omega)}^* - \hat{s}_{21(j\omega)}^*). \tag{6}$$

By this procedure, the first-order sensitivities are obtained directly. This is valid for the additional network elements, too.

Assuming approximately equal experimental accuracy for all four s parameters, the weight functions $W_{i(j\omega)}$ of (7) allow a fast optimization procedure:

$$W_{i(j\omega)} = \frac{1}{\mid \hat{s}_{ij(j\omega)} \mid^n}. \tag{7}$$

In [2] the nodal voltages are differentiated with respect to the 2-terminal admittance Y_k. If the relation (8) is applied, the sensitivities for the different network elements are obtained:

$$\frac{\partial \parallel \boldsymbol{Y}_b \parallel}{\partial El} = \frac{\partial \parallel \boldsymbol{Y}_b \parallel}{\partial Y_k} \frac{\partial Y_k}{\partial El} \tag{8}$$

where Y_k is the 2-terminal branch admittance; $\parallel \boldsymbol{Y}_b \parallel$ is the branch admittance matrix;

$$\frac{\partial \parallel \boldsymbol{v}_n \parallel}{\partial El} = - \parallel \boldsymbol{Y}_n \parallel^{-1} \parallel \boldsymbol{A} \parallel \frac{\partial \parallel \boldsymbol{Y}_b \parallel}{\partial Y_k} \frac{\partial Y_k}{\partial El} \cdot \left\| \parallel \boldsymbol{v}_b \parallel - \parallel \boldsymbol{e}_b \parallel \right\| \tag{9}$$

$\parallel \boldsymbol{Y}_n \parallel$ is the nodal admittance matrix; $\parallel \boldsymbol{e}_b \parallel$ is the independent branch voltage vector; $\parallel \boldsymbol{v}_n \parallel$ is the nodal voltage vector; $\parallel \boldsymbol{v}_b \parallel$ is the branch voltage vector; $\parallel \boldsymbol{A} \parallel$ is the reduced incidence matrix. The formula for the transadmittance elements is obtained by omitting the vector $\parallel \boldsymbol{e}_b \parallel$. With a suitable tree configuration $\partial I_1'/\partial El$ and $\partial I_2'/\partial El$ of (3) and (4) are obtained by dividing (9) by the characteristic impedance Z_0.

The following comparison is based on the first-order sensitivity calculation of the error function, formed by using all four s parameters at a single frequency value. Furthermore, it is based on the Gaussian elimination process and the traditional matrix inversion. Sparse matrix solutions are not considered. As the multiplication and division operations occupy most of the computer time, only these operations are compared. Applying the method [2], it is advantageous to execute the matrix inversion $\parallel \boldsymbol{Y}_n \parallel^{-1}$ already at the beginning, since this matrix is used for the gradient calculation of (9). The traditional matrix inversion requires at least $(n^3 + 2n^2)$ essential operations. One operation is defined as either one multiplication and addition or one division. n is the number of network equations. As the process is only applied to two nodal voltage sensitivities at both ports of the original network, the number of additional operations is small compared with $(n^3 + 2n^2)$.

With procedure [1], Gaussian elimination [11] may be applied. In [12] it is shown that for the original network and its adjoint network only k_1 operations are used:

$$k_1 = \tfrac{1}{3}n(n^2 - 1) + 2n^2. \tag{10}$$

For the second original network (Fig. 3) only the excitations are different from the first configuration. For this reason, only $(2n^2)$ further operations are needed for the sensitivity calculation with respect to the error function of all four s parameters:

$$k_2 = k_1 + 2n^2 = \tfrac{1}{3}n(n^2 - 1) + 4n^2. \tag{11}$$

At large values of n, the second method takes much more computer time.

If the first- as well as the second-order sensitivities have to be calculated, the method by Downs [16] is more favorable than [1]. Only k_3 operations are used with [16]:

$$k_3 = n^3 + 2m + 5m^2 \tag{12}$$

where m is the number of branch admittances for which the first- as well the second-order sensitivities are used. However, in this case, the procedure [2] is comparable with [16]. Especially with respect to the scattering parameters, further efficient sensitivity calculations are given in [18]–[21].

At the end of this section, it has to be mentioned that the Gaussian elimination is not optimal [13]. In [13] a special procedure for matrix inversions is given, allowing less arithmetical operations. But the said procedure is favorable at approximately $n > 1000$.

IV. Discussion of the Numerical Results for the Small-Signal s Parameters

With the numerical values of Table I for the emitter configuration, the calculated s parameters of Figs. 4 and 5 are obtained. In the same figures, the measured s parameters are given. The remaining errors between the measured and calculated quantities are caused mainly by the phase angles of these parameters. These differences are partly due to the assumed package equivalent circuit. At shorter wavelengths, taking into account the package dimensions, the determination of an accurate equivalent circuit with lumped elements becomes more problematic. Such a network can only be valid over a limited frequency range and its values are more formal than physical. An ideal lossless transmission line piece of the length l can be replaced by an equivalent circuit containing one L and one C if $\tanh \gamma l \approx \gamma l$. γ is the transmission line constant per unit length. The ratios of the effective wavelengths to the dimensions of the active part of the transistor pill are more favorable, because the latter dimensions amount to only some microns. Nevertheless, the pill's equivalent circuit elements may also be frequency depend-

TABLE I
NUMERICAL ELEMENT VALUES FOR THE TRANSISTOR AT-561 AT THE BIAS CONDITION (I_C = 3 mA; U_{CE} = 10 V) (SEE FIG. 2)

C_1	= 0.127 (pF)	L_1	= 0.105 (nH)	R_{b1}	=	12.92	(Ω)
C_2	= 0.093	L_2	= 0.182	R_{b2}	=	5.48	
C_3	= 0.059	L_3	= 0.215	$R_{b'e'}$	=	304.74	
C_4	= 0.102	L_4	= 0.168	R_{TR}	=	8.56	
C_5	= 0.022	L_5	= 0.150				
C_{ci}	= 0.123	L_6	= 0.216				
C_{co}	= 0.077	L_{TR}	= 0.208				
$C_{b'e'}$	= 2.250						

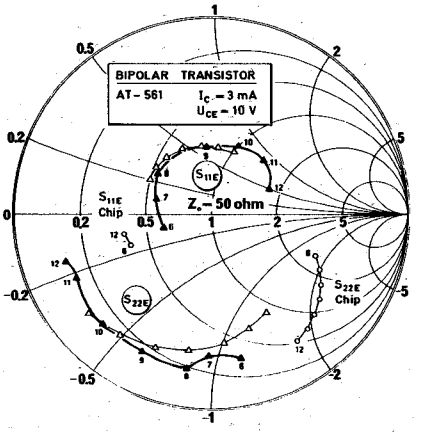

Fig. 4. Scattering parameters s_{11} and s_{22} (transistor AT-561; I_C = 3 mA; U_{CE} = 10 V; reference planes—base side at the package edge, collector side 0.625 mm away from the package edge). ▲—measured; △—calculated; ○—parameters of the chip alone (calculated).

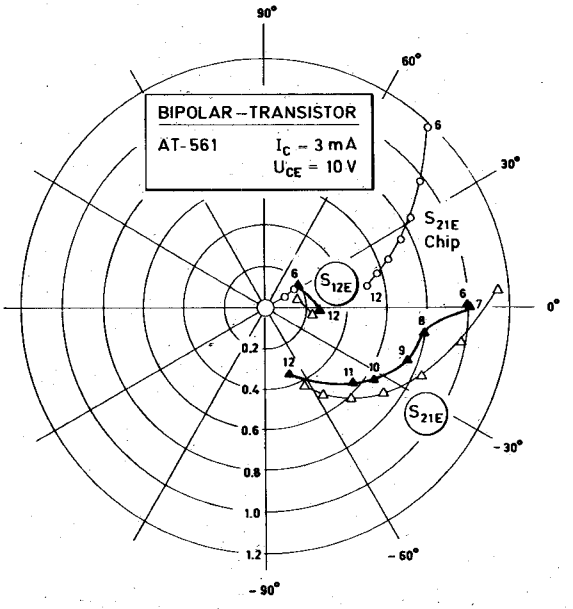

Fig. 5. Scattering parameters s_{21} and s_{12} (see caption of Fig. 4).

ent for other reasons. As an example, it is shown in [14] that at heavier grading of impurity concentration in the base region, the lumped base-emitter capacitance $C_{b'e'}$ (Fig. 2) is more frequency dependent. An improvement of the agreement could be achieved by the subdivision of this capacitance $C_{b'e'}$ (Fig. 6).

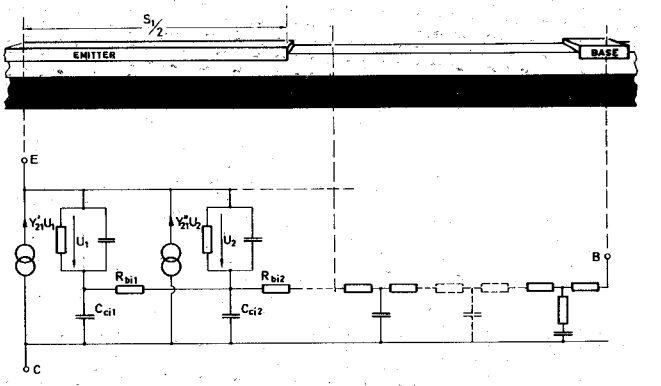

Fig. 6. Extension of the lumped equivalent circuit of the one-dimensional transistor chip to a lumped equivalent circuit of a two-dimensional chip.

The small-signal s parameters of the chip alone have also been calculated (Figs. 4 and 5). This chip modeling can be made more precise by considering the two dimensional (Fig. 6) or even the three-dimensional character of the transistor. But, by the application of an increasing number of network elements, applying computer optimization, the possibility exists of finding element values without true physical meaning. Therefore, in this case, the physical limits and starting values have to be estimated very carefully.

Fig. 7 shows the calculated dependence of the complex transadmittance $Y_{21e'}$. Furthermore, the calculated values of $Y_{21e'}$ with respect to [14] are shown in the same figure. These values have been calculated, assuming a frequency f_{Ti} of 7 GHz [15] and $\eta = ln(N_{BE}/N_{BC}) = 4$ (N_{BE},N_{BC} = impurity concentrations at the emitter and collector edge of the base). For $\eta \neq 4$ and for f_{Ti} slightly different from 7 GHz the agreement is not better than with $\eta = 4$ and $f_T = 7$ GHz. In this frequency range, a precise measurement for the experimental confirmation of either curve is difficult, especially beyond the 6-dB-per-octave falloff region of $|h_{fe}|$ [15]. A certain discrepancy for the result based on [14] can be explained with [15]. The base impurity concentration increases with depth in the compensation region, resulting in a locally retarding field. In [14], this point has not been considered. Furthermore, a better model of the base-emitter admittance with more elements results in a better model for the transadmittance.

In Table II the influence of different chip elements on

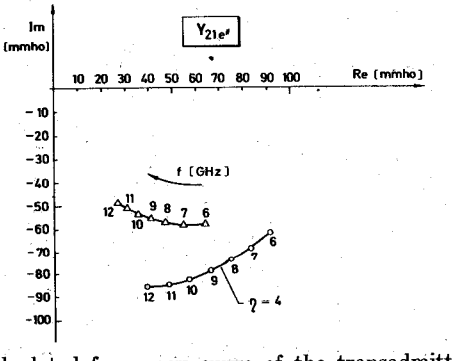

Fig. 7. Calculated frequency curve of the transadmittance Y_{21e}. △ = Y_{21e} obtained with the additional network (Fig. 2). ○ = Y_{21e} obtained with [14].

TABLE II
INFLUENCE OF THE NETWORK ELEMENTS ON MSG' AND K' FOR 50-PERCENT REDUCTION IN THE NETWORK ELEMENT

		R_{bl}	R_{TH}	C_{ci}	C_{co}	$C_{b'e'}$	Package	Rel. Change
f(GHz)	6.0	+ 0.2	-18.5	-12.3	+11.3	-19.0	+14.0	$100.\frac{\Delta K'}{K'}$
	8.0	+ 8.9	-21.4	-15.0	+13.9	-13.3	+17.5	
	10.5	+ 8.4	-25.2	-16.2	+10.9	- 3.2	+25.2	
f(GHz)	6.0	+23.3	+18.0	+10.1	+45.7	+4.9	+24.4	$100.\frac{\Delta MSG'}{MSG'}$
	8.0	+37.0	+11.0	+ 5.9	+47.2	+9.9	+20.2	
	10.5	+112.0	+68.9	+52.6	+114.0	+58.3	+87.3	

the calculated maximum stable gain (MSG') and the stability factor K' at three frequency values is shown. The relative changes of MSG' and K' have been calculated at an individual 50-percent reduction of the corresponding elements. Only one network element value has been changed at a time. The package influence has been eliminated completely in the last column of Table II. This package reduces gain and stability. A comparison of the element values of AT-101A [5] shows that the improvement is based on smaller capacitance values and a larger $|Y_{21e'}|$. But the total base resistance of this more recent transistor is now larger, above 6 GHz.

V. Discussion of the Noise Calculations

In Fig. 2 the noise sources were also introduced. m_E considers the generation-recombination noise with respect to the base-emitter junction [25]. This factor m_E can be approximately determined with the corresponding dc characteristic. The transistor AT-561 shows a factor m_E of $\approx$1.03 at $U_{CE} = 10$ V and $I_C = 3$ mA. For frequencies above 6 GHz, the influence of the generation-recombination noise is small compared with the contribution of the collector shot noise.

In Table III the calculated absolute noise figures F_{opt}' and the calculated optimal source admittance Y_{opt}' [7] are compared with the corresponding measured values F_{opt} and Y_{opt}. It can be seen that the better the modeling of the s_{11} parameter, the better the agreement of Y_{opt}' and F_{opt}' with Y_{opt} and F_{opt}. One reason for the remaining error may be that at $I_C = 3$ mA, high current injection phenomena can set in. In this frequency range, the contribution of the thermal noise sources i_{Rb1} and i_{Rb2} is smaller than that of the correlated noise sources i_{nb} and i_{nc}. The simulation of the fourth noise parameter R_n is not satisfactory. As an example, at 6 GHz, 25 Ω instead of 48 Ω have been calculated. In this connection, it has to be said that R_n is determined by (13):

$$R_n = \frac{(F - F_{opt})G_s}{(G_s - G_{s\,opt})^2 + (B_s - B_{s\,opt})^2}$$

$$Y_s = G_s + jB_s = \text{source admittance.} \qquad (13)$$

From (13) it can be seen that R_n is extremely sensitive to changes of G_s and B_s. In Table IV the influence of different chip and package elements is shown. The relative changes of F_{opt}' have been calculated as described in Section IV [22]–[24].

TABLE III
CALCULATED AND MEASURED OPTIMAL NOISE FIGURES AND OPTIMAL SOURCE ADMITTANCES AS A FUNCTION OF FREQUENCY

f (GHz)	F'_{opt}	F_{opt}	Y'_{opt} (mmho)	Y_{opt} (mmho)
6.0	4.89	3.55	25.5+4.0j	29.6+6.4j
8.0	5.99	5.50	25.0+5.5j	28.0+8.4j
10.5	10.29	13.58	18.5+9.5j	12.0+3.6j

TABLE IV
INFLUENCE OF THE NETWORK ELEMENTS ON THE OPTIMAL NOISE FIGURE F_{OPT}' AT 10.5 GHz FOR A 50-PERCENT REDUCTION IN THE NETWORK ELEMENT

Element	R_{bl}	R_{TH}	C_{ci}	C_{co}	$C_{b'e'}$	Package
$100.\frac{\Delta F'_{opt}}{F'_{opt}}$	- 8.7	-41.7	+2.1	+18.7	-63.2	-15.6

VI. Conclusion

An equivalent circuit for a microwave bipolar transistor up to 12 GHz has been shown. At these high frequencies, the equivalent circuit for the package is more formal than physical. A better agreement between measured and calculated values could mainly be achieved by a subdivision of the base-emitter admittance in more elements. The influence of a new rugged metal–ceramic package as well as the influence of different chip equivalent circuit elements on gain, stability, and noise have been shown in detail. With microwave bipolar transistors, high-current injection phenomena set in at relatively low currents. In a further work it would be interesting to examine the contribution of these effects at larger current densities [26]. In connection with the computerized optimization, three different sensitivity calculations have been examined, considering several new aspects of computer calculations.

References

[1] S. W. Director and R. A. Rohrer, "Automated network design—The frequency-domain case," *IEEE Trans. Circuit Theory*, vol. CT-16, pp. 330–337, Aug. 1969.

[2] P. J. Goddard and R. Spence, "Efficient method for the calculation of first- and second-order network sensitivities," *Electron. Lett.*, vol. 5, pp. 351–352, Aug. 1969.

[3] K. Hartmann and M. J. O. Strutt, "Scattering and noise parameters of four recent microwave bipolar transistors up to 12 GHz," *Proc. IEEE* (Lett.), vol. 61, pp. 133–135, Jan. 1973.

[4] P. A. Villalaz, "Theory and techniques of sensitivity applied to electrical device modeling and circuit design," Ph.D. dissertation, Imperial College, Univ. London, London, England, Sept. 1972.

[5] K. Hartmann, W. Kotyczka, and M. J. O. Strutt, "Computer-aided determination of the small-signal equivalent network of a bipolar microwave transistor," *IEEE Trans. Microwave Theory Tech.*, vol. MTT-20, pp. 120–126, Feb. 1972.

[6] ——, "Equivalent networks for three different microwave bipolar transistor packages in the 2–10 GHz range," *Electron. Lett.*, vol. 7, pp. 510–512, July 1971.

[7] W. Baechtold, W. Kotyczka, and M. J. O. Strutt, "Computerized calculation of small signal and noise properties of microwave transistors," *IEEE Trans. Microwave Theory Tech.* (*Special Issue on Computer-Oriented Microwave Practices*), vol. MTT-17, pp. 614–619, Aug. 1969.

[8] S. D. Malaviya and A. van der Ziel, "A simplified approach to noise in microwave transistors," *Solid-State Electron.*, vol. 13, pp. 1511–1518, 1970.

[9] W. Kotyczka, "Small signal, stability and noise behavior of microwave bipolar transistors in the S and C band" (in German), Ph.D. dissertation 4730, Swiss Federal Institute of Technology, Zurich, Switzerland, 1971.

[10] H. J. Butterweck, "Orthogonal Kirchhoff modes—A new tool of network analysis," *IEEE Trans. Circuit Theory*, vol. CT-19, pp. 307–312, July 1972.
[11] E. Stiefel, *Introduction to the Numerical Mathematics* (in German). Stuttgart, Germany: Teubner, 1965, p. 21.
[12] S. W. Director, "*LU* factorization in network sensitivity computation," *IEEE Trans. Circuit Theory* (Corresp.), vol. 18, pp. 184–185, Jan. 1971.
[13] V. Strassen, "Gaussian elimination is not optimal," *Numer. Math.*, vol. 13, pp. 354–356, 1969.
[14] J. te Winkel, "Drift transistor, simplified electrical characterization," *Electron. Radio Eng.*, pp. 2–10, Aug. 1959.
[15] H. F. Cooke, "Microwave transistors: Theory and design," *Proc. IEEE (Special Issue on Microwave Semiconductors)*, vol. 59, pp. 1163–1181, Aug. 1971.
[16] T. Downs, "An approach to the computation of network sensitivities," *Marconi Rev.*, 3rd qr., pp. 205–212, 1972.
[17] J. W. Bandler and R. E. Seviora, "Current trends in network optimization," *IEEE Trans. Microwave Theory Tech. (1970 Symposium Issue)*, vol. MTT-18, pp. 1159–1170, Dec. 1970.
[18] ——, "Wave sensitivities of networks," *IEEE Trans. Microwave Theory Tech.*, vol. MTT-20, pp. 138–148, Feb. 1972.
[19] ——, "Direct method for evaluating scattering matrix sensitivities," *Electron. Lett.*, pp. 773–774, 1970.
[20] V. A. Monaco and P. Tiberio, "On linear network scattering matrix sensitivity," *Alta Freq.*, vol. 39, pp. 193–195, Feb. 1970.
[21] G. Iuculano, V. A. Monaco, and P. Tiberio, "Network sensitivities in terms of scattering parameters," *Electron. Lett.*, pp. 53–55, Jan. 1971.
[22] K. Hartmann and M. J. O. Strutt, "Changes of the four noise parameters due to general changes of linear two-port circuits," *IEEE Trans. Electron Devices*, vol. ED-20, pp. 874–877, Oct. 1973.
[23] K. Hartmann, "The small signal and noise behavior of microwave bipolar transistors up to 12 GHz," in *Proc. European Microwave Conf.* (Brussels, Belgium, Sept. 4–7, 1973).
[24] K. Hartmann, W. Kotyczka, and M. J. O. Strutt, "Computerized determination of electrical network noise due to correlated and uncorrelated noise sources," *IEEE Trans. Circuit Theory* (Short Paper), vol. CT-20, pp. 321–322, May 1973.
[25] B. Schneider and M. J. O. Strutt, "Theory and experiments on shot noise in silicon *P-N* junction diodes and transistors," *Proc. IRE*, vol. 47, pp. 546–554, Apr. 1959.
[26] ——, "Shot and thermal noise in germanium and silicon transistors at high-level current injections," *Proc. IRE*, vol. 48, pp. 1731–1739, Oct. 1960.
[27] K. Hartmann, "Computer simulation of linear noisy two-port circuits with special consideration of the bipolar transistor up to 12 GHz." (in German), Ph.D. dissertation 5118, Swiss Federal Institute of Technology, Zurich, Switzerland, 1973.

A Theoretical Study of the High-Frequency Performance of a Schottky-Barrier Field-Effect Transistor Fabricated on a High-Resistivity Substrate

GARY D. ALLEY, MEMBER, IEEE, AND HARRY E. TALLEY, SENIOR MEMBER, IEEE

Abstract—**The short-circuit admittance parameters for a silicon Schottky-barrier field-effect transistor (SBFET) fabricated on a high-resistivity substrate are calculated from first principles ignoring the effects of minority carriers. The calculations show the maximum frequency of oscillation for a device with a 1-μm gate to be 17.9 GHz, neglecting the parasitics associated with the contact metallizations, and 14.7 GHz when the parasitics are included.**

In order to describe the dynamic behavior of the device, the static properties must first be obtained. The simultaneous solution of Poisson's equation and the continuity equation, both in two dimensions, gives the static charge and potential distribution in the device. The effects of a field-dependent mobility are included in the continuity equation. Using the results of static two-dimensional solutions, a one-dimensional device model is developed that permits the dynamic device behavior to be described by a one-dimensional linear ordinary differential equation. By solving this equation under appropriate boundary conditions, the device y parameters are found as functions of frequency. Calculated results are shown to be in good agreement with published experimental data.

Manuscript received July 3, 1973; revised November 9, 1973. This work is based on a paper presented at the 1972 IEEE International Electron Device Meeting, Washington, D. C., Dec. 4–6, 1972.

G. D. Alley was with the Department of Electrical Engineering, University of Kansas, Lawrence, Kans. He is now with Bell Laboratories, North Andover, Mass.

H. E. Talley is with the Department of Electrical Engineering, University of Kansas, Lawrence, Kans.

I. Introduction

THE DEMONSTRATED high-frequency capabilities of field-effect transistors [1] indicate that they will have important applications in microwave systems. In this paper we present a method for calculating the y parameters as a function of frequency for a silicon Schottky-barrier field-effect transistor (SBFET) [2]. The results of these calculations are valid up to and beyond the maximum frequency of oscillation for a given device, so that the method may be used to optimize the high-frequency response of an SBFET. The theoretical calculations presented are compared with experimental data published in the literature and are shown to be in good agreement.

In order to obtain the desired y parameters, we first solve simultaneously the continuity equation and Poisson's equation, both in two dimensions, in order to find the